6-1-2017

Inhibition of MT1-MMP proteolytic function and ERK1/2 signalling influences cell migration and invasion through changes in MMP-2 and MMP-9 levels

Mario A. Cepeda
Western University

Caitlin L. Evered
Western University

Jacob J.H. Pelling
Western University

Sashko Damjanovski
Western University, sdamjano@uwo.ca

J. Cell Commun. Signal. (2017) 11:167–179
DOI 10.1007/s12079-016-0373-3

RESEARCH ARTICLE

Inhibition of MT1-MMP proteolytic function and ERK1/2 signalling influences cell migration and invasion through changes in MMP-2 and MMP-9 levels

Mario A. Cepeda [1] · Caitlin L. Evered [1] · Jacob J. H . Pelling [1] · Sashko Damjanovski [1,2]

Received: 31 October 2016 / Accepted: 19 December 2016 / Published online: 9 January 2017

Abstract Membrane type-1 matrix metalloproteinase (MT1-MMP, MMP-14) is a unique protease that cleaves extracellular proteins, activates proMMPs, and initiates intracellular signalling. MCF-7 cells are non-invasive and deficient in MT1-MMP, MMP-2, and MMP-9 expression. We created an MCF-7 cell line (C2) that stably produces active MT1-MMP and demonstrated increased ERK1/2 phosphorylation. MAPK inhibition in this cell line showed an inverse relationship in MMP-2 and MMP-9 transcripts where levels of these genes increased and decreased, respectively. Using invasive MDA-MB 231 cells that endogenously produce MT1-MMP and have naturally high pERK levels, we demonstrated the identical inverse relationship between MMP-2 and -9 transcript and protein levels, suggesting that this novel relationship is conserved amongst MT1-MMP positive breast cancer cells. To further analyze the relationship between MMP-2 and -9 levels, we chemically inhibited activation and catalytic activity of MT1-MMP using a furin and MMP inhibitor, respectively, to show that interference with the functions of MT1-MMP induced changes in MMP-2 and 9 transcript levels that were always inverse of each other, and likely mediated by differential transcriptional activity of the NF-κB transcription factor. Furthermore, we analyzed the functional consequences of these expression changes to show MMP, and in particular ERK, inhibition decreased migration and invasion using 2D culture, and inhibits the formation of an invasive phenotype in Matrigel 3D culture. This study demonstrated a novel inverse transcriptional relationship between MMP-2 and -9 levels and MT1-MMP activity that have functional consequences, and also showed that increases in the levels of MMPs does not necessarily correlate with an invasive phenotype.

Keywords MT1-MMP · MMP-2 · MMP inhibition · Cell migration · 3D culture · ERK signalling

Mario A. Cepeda and Caitlin L. Evered are Co-First Authors

✉ Sashko Damjanovski
sdamjano@uwo.ca

[1] Department of Biology, Faculty of Science, University of Western Ontario, BGS room 3053, 1151 Richmond St N, London, ON N6A 5B7, Canada

[2] Lawson Health Research Institute, London, ON, Canada

Introduction

Matrix metalloproteinase 14 (MMP-14), also known as membrane type-1 (MT1)-MMP, is unique amongst the family of MMPs due to its unique regulation of cell movement. Cell migration in multicellular organisms requires passage between cells and through the extracellular matrix (ECM). Such cell migration through a barrier, termed invasion, is often protease dependent (Bateman et al. 2009; Järveläinen 2009). Cell invasion is fundamental during embryogenesis and plays a critical role in adult wound healing, pregnancy, and disease (Bourboulia and Stetler-Stevenson 2010). The roles played by cytoskeletal and cell adhesion molecules in cell movement have been well described by many in vitro assays, but those played by MMPs are confounding (Lambert et al. 2004). The activity of potent MMPs, such as gelatinases MMP-2 and -9, cleaves ECM proteins and thus it was believed facilitated cell movement (Klein and Bischoff 2011). The enzymatic activity of MMPs is in turn inhibited by a family of four secreted inhibitors, the tissue inhibitors of MMPs (TIMPs) (Lambert et al. 2004). The interactions of MMPs and TIMPs are complex and need to be tightly regulated as they have functions beyond ECM remodelling, including roles in the cell signalling and morphology changes needed for cell movement (Frantz et al.

2010; Hynes and Naba 2012). Here we examine MT-1 MMP's role in orchestrating these many cellular functions.

To date, 24 MMPs have been identified in vertebrates that together can cleave all components of the ECM, but MMP enzymatic activity alone is not enough to facilitate invasion (Hotary et al. 2006; Sabeh et al. 2009). All MMPs are synthesized as inactive zymogens, proMMPs, whose activation requires the removal of the N-terminal pro-domain. Membrane-type MMPs, including MT1-MMP, are activated intracellularly, with activation in the trans-Golgi principally by furin through a protein-convertase-dependent mechanism (Seidah et al. 2008). MT1-MMP is anchored at the cell membrane in an active form (Sternlicht and Werb 2001), whereby secreted proMMPs, such as the gelatinases, are activated extracellularly by other, already active proteinases, including membrane tethered MT1-MMP. Active membrane bound MT1-MMP is involved in a well described mechanism that activates proMMP-2. This requires the formation of the MT1-MMP/TIMP-2/proMMP-2 complex, where MT1-MMP is in the correct orientation to cleave the pro-peptide domain of proMMP-2 and release the activated MMP-2 into the ECM (Itoh et al. 2001; Lehti et al. 2000). Additionally, the MT1-MMP/TIMP-2/MMP-2 complex has been shown to subsequently activate secreted proMMP-9 (Toth et al. 2003). Thus MT1-MMP is involved in a well described functional relationship with MMP-2 and MMP-9, and as such a mechanism that correlates their expression levels likely exist.

Cell-surface MT1-MMP and TIMP-2 can also form an additional receptor/ligand complex whereby MT1-MMP initiates the MAPK pathway, leading to downstream phosphorylation of extracellular signal-regulated kinase (ERK1/2) (Pahwa et al. 2014; Sounni et al. 2010). Our previous work demonstrated that optimal levels of active MT1-MMP, not just a global increase in MT1-MMP protein levels, are required for elevated pERK levels (Cepeda et al. 2016). The localization of MT1-MMP by its cytosolic C-terminal domain also plays a role in both gelatinase activation and cell signalling. Membrane localization of MT1-MMP by its cytosolic domain is also important in the regulation of cell migration and invasion as, together with cortactin, is localized to invadopodia - cell membrane protrusions that serve as focal sites of ECM degradation (Poincloux et al. 2009). MT1-MMP is thus perfectly poised to localize, and co-ordinate, ECM degradation and cell signalling activity in cells situated to migrate or invade.

To investigate the contributions played by MT1-MMP in regulating MMP-2 and MMP-9 transcript levels we used MCF-7 and MDA-MB-231 cells and examined the effects of altered MT1-MMP activation, MMP catalytic activity, and ERK1/2 signalling (using furin inhibitor, BB94, and U0126, respectively). Regardless of treatment, transcript levels of the two gelatinases, MMP-2 and MMP-9, were always altered in an inverse relationship. Functional analysis of these changes in MMP levels was examined and only U0126 treatment, but not BB94 treatment, decreased cell migration as seen by scratch and transwell assays. However, both U0126 and BB94 treatment decreased cell invasion through a Matrigel transwell assay, as well as the number of cell protrusions in Matrigel 3D culture.

Materials and methods

Cell culture conditions

Human cell lines used are MCF-7 (ATCC® HTB-22™) and MDA-MB-231 (ATCC® HTB-26™). The three MCF-7 breast cancer cell lines that stably overexpress MT1-MMP were generated as previously describe (Cepeda et al. 2016) - C1, expressed ~2500 fold increase in MT1-MMP mRNA compared to MCF-7 parental cells, C2 ~ 1100 fold and C3 an ~11 fold increase. Cells were cultured in Dulbecco's Modified Eagles (DMEM)/F-12 medium (Thermo Fisher) supplemented with 10% fetal bovine serum (FBS), 100 IU/mL penicillin, 100 μg/mL streptomycin, in a humidified incubator at 37 °C and 5% CO_2. Cells were maintained under 80% confluency and passaged accordingly using 0.25% Trypsin-EDTA (Thermo Fisher).

Chemical inhibitors

The following inhibitors were used: U0126 (Santa Cruz Biotechnology) which provided noncompetitive inhibition with respect to ERK and ATP substrates (DeSilva et al. 1998). BB-94 (Santa Cruz Biotechnology) is an MMP substrate analog that binds to and inhibits the zinc ion in the MMP catalytic site (Low et al. 1996). Furin Inhibitor I (Millipore) binds the catalytic site of furin, blocking activity (Coppola et al. 2008). Concentrations of respective inhibitors were as follows: U0126 10 μM (Assent et al. 2015; D'Alessio et al. 2008), BB-94 10 μM (Itoh et al. 2001; Mori et al. 2002), and Furin Inhibitor I 5 μM, 10 μM, and 20 μM.

RNA extraction and quantitative real-time PCR

Cells were seeded at a density of 1×10^6 cells/mL in 35 mm cell culture plates (Corning) in 2 mL of DMEM/FBS medium and were treated with U0126 (10 μM), BB-94 (10 μM), Furin inhibitor I (5, 10, 20 μM), or DMSO (0.1%) for 24 h, lysed, and RNA was collected using the RNeasy Kit (Qiagen). cDNA was synthesized from 1 μg of RNA using qScript cDNA supermix (Quanta). The relative mRNA levels of MT1-MMP, MMP-2, MMP-9, and TIMP-2 were assayed by qPCR using SensiFAST SYBR No-ROX Kit (FroggaBio) and the CFX Connect™ Real-Time PCR Detection System (Bio-Rad). mRNA levels were quantified by the ΔΔCT method and displayed as fold change relative to MCF-7 or MDA-MB-

231 breast cancer cells under normal culture conditions. The level of glyceraldehyde 3-phosphate dehydrogenase (GAPDH) mRNA was used as the internal control. Primer sequences used were as follows;

MT1-MMP 5′-GCAGAAGTTTTACGGCTTGCA 5′- TCGAACATTGGCCTTGATCTC
MMP-2 5′- AGCTCCCGGAAAAGATTGATG 5′-CAGG GTGCTGGCTGAGTAGAT
MMP-9 5′-CCTGGAGACCTGAGAACCAATC 5′-GATT TCGACTCTCCACGCATCT
TIMP-2 5′-'CGACATTTATGGCAACCCTATC 5'-GCCGTGTAGATAAACTCTATATCC
GAPDH 5′-ACCCACTCCTCCACCTTTGA 5′-CTGT TGCTGTAGCCAAATTCGT

Protein collection and immunoblotting

Cells were seeded and treated as with qPCR analysis. Following 24 h of treatment cell lysates were collected and total protein concentration was determined. Protein aliquots (15 μg) were analyzed by immunoblotting with MT1-MMP, β-actin, pERK or total ERK1/2 primary antibodies, followed by incubation with the appropriate secondary HRP-conjugated antibody and detected using SuperSignal West Pico chemiluminescent substrate (Thermo Fisher). Incubation with primary antibodies occurred overnight at 4 °C, and secondary antibodies for one hour at room temperature. Primary antibodies used were: Human MT1-MMP (1:1000, AB6004, Millipore), pERK (1:2000, D13.14.4E), total ERK1/2 (1:2000, 137F5) (Cell Signalling Technology), and β-Actin (1:1000, C4). Goat anti-mouse IgG (H + L) (Bio-Rad) and goat anti-rabbit IgG (H + L) (Thermo Fisher) HRP conjugates were used as secondary antibodies (1:10,000). Images were captured using the Molecular Imager® ChemiDocTM XRS System (BioRad). Quantitative densitometric analysis of immunoblots was performed using QuantityOne software (Bio-Rad). Band intensity was obtained for the MT1-MMP, β-Actin, phospho-ERK and total ERK1/2 signal of each sample from three independent biological experiments. MT1-MMP pro- and active protein is presented as a ratio between each respective band intensity and β-Actin signal. ERK1/2 activation is presented as a ratio between pERK and total ERK1/2 band intensity normalized to cells under control conditions.

Generation of proMMP-2 containing conditioned medium

ProMMP-2 conditioned medium (Cepeda et al. 2016) was used to verify the efficiency of BB-94 in preventing activity of MMPs of cleaving substrate as determined by gelatin zymography analysis. In brief, conditioned medium (CM) containing proMMP-2 protein was created by transfecting MCF-7 breast cancer cells with a cDNA construct coding for MMP-2 protein. Since MCF-7 cells are MT1-MMP and MMP-2 deficient, proMMP-2 CM generated in this way results in CM that contains predominately proMMP-2 protein. Following a 24-h incubation period post transfection, cells were washed with phosphate buffered saline (PBS) and incubated in serum free DMEM/F12 media for 24 h. This medium conditioned with the soluble proMMP-2 product was then collected, aliquoted, and stored at −80 °C for later use.

Gelatin zymography and reverse gelatin zymography

Gelatin zymography was performed as previously described (Toth et al. 2001) and used to compare the levels of secreted pro- and activate MMP-2 and MMP-9 in the medium of cells following treatment with DMSO (0.1%), U0126 (10 μM), or BB-94 (10 μM). Briefly, 15 μL of medium was loaded on a 10% polyacrylamide-0.1% gelatin gel and subjected to electrophoresis. After electrophoresis, the gels were incubated in renaturing buffer (25% *v*/v Triton X-100 in dH2O), and then incubated in developing buffer (0.5 M Tris–HCl, pH 7.8, 2 M NaCl, 0.05 M CaCl2, and 0.2% Brij 35) at 37 °C for 48 h to allow the MMPs to cleave the gelatin embedded within the polyacrylamide gel. The gel was then stained with a 0.5% Coomassie blue, 5% methanol, 10% acetic acid solution, and progressively destained with a 20% methanol, 10% acetic acid solution until bands that represent cleaved gelatin were clearly visible. Images were taken using the Molecular Imager® ChemiDocTM XRS (BioRad). Reverse zymography, which measures TIMP-2 activity, was performed by adding proMMP-2 conditioned medium to the 10% polyacrylamine-0.1% gelatin gel lacking denaturing detergents. Protein loading, renaturing, and staining process are identical to gelatin zymography, however in reverse zymography when the gel is de-stained it is clear, except for dark blue banding that represents TIMP-2 proteins bound to MMPs embedded in the gel, preventing their activity and protecting the gelatin in that location.

Firefly luciferase transcriptional activity assay

Transcriptional activity of AP-1 and NF-κB was examined in cells following inhibitor treatments. In brief, MCF-7, C2, and MDA-MB-231 cells were seeded at a density of 3.0×10^4 cells/well in a 96-well culture plate (Corning) and incubated for 24 h. Following incubation, cells were transfected using Lipofectamine 2000 (Thermo Fisher), according to the manufacturer's instructions, with luciferase reporter plasmids. Either 0.2 μg of mammalian 3xAP1pGL3 (Addgene Plasmid # 40342 for AP-1 transcription, or p1242 3xKB-L (Plasmid #26699) for NF-κB transcription, were transfected into cells. 24 h post transfection cells were subjected to

treatment with DMSO (0.1%), U0126 (10 μM), or BB-94 (10 μM). 12 h later cells were lysed and treated with Firefly Luciferase Glow Assay reagents (Thermo Fisher) according to the manufacturer's instructions. Luminescence was detected using ModulusTM II Microplate Multimode Reader and the GloMax®- Multi Detection System with Instinct® Software.

Scratch wound closure migration assay

To examine the effects of respective inhibitor treatment on cell migratory potential, MDA-MB-231 breast cancer cells were seeded at a density of 2.5×10^5 cells/mL in a 35 mm cell culture dish (Corning) in 2 mL of DMEM/FBS medium and allowed to form a monolayer for 24 h. Following incubation, medium was aspirated and the monolayer was disrupted using a 1000 μL pipette tip to create a wound down the length of the culture dish. The remaining adhered cells were washed three times with PBS (pH 7.2) to remove cell debris and then incubated with fresh DMEM 10% FBS, 1% pen/strep medium containing treatment of DMSO (0.1%), U0126 (10 μM), BB-94 (10 μM), or Furin Inhibitor I (20 μM). 2 h post wound generation, using the Zeiss Observer. A1 AX10 microscope, 10 images were captured down the length of the scratch that represent the 'initial' size of the wound for each respective sample. The same area of the wound was imaged at 6, 12, and 24 h following wound healing to examine the ability to migrate into the wound space. Scratch closure was quantified by measuring the width of the scratch each day and normalizing it to the initial size of the scratch. Scratch closure is presented as a mean percentage of the initial scratch size ± SEM.

Transwell cell motility assays

The migratory and invasive potential of MDA-MB-231 cells was measured using 24-well 8 μm pore transwell inserts (Corning). 2.0×10^4 cells were seeded on the upper chamber of the transwell in serum-free medium treated with DMSO (0.1%), U0126 (10 μM), or BB-94 (10 μM). Treated cells were allowed to migrate (24 h) or invade (48 h) towards the bottom chamber which contained DMEM/F-12 medium supplemented with 10% FBS serving as the chemoattractant. Migration assays were performed with uncoated transwell inserts, whereas invasion assays were performed with inserts coated with 20% Matrigel (BD Biosciences). Cells that migrated to the lower chamber of the transwell insert were fixed, stained, and quantified as per Marshall, 2011. For quantification of invasion transwells, cells were fixed with 100% methanol and cells that did not invade through the transwell insert and residual Matrigel were removed from the upper membrane surface with a damp cotton swab. Invaded cells were then stained with a 0.5% crystal violet solution. Cells were then imaged and 15 images were blindly taken per transwell and quantified using ImageJ software (NIH, Bethesda).

Three dimensional (3D) cell culture

MDA-MB-231 cells were embedded in 50% Matrigel matrix (BD Biosciences) and processed for fluorescent staining to assess changes in invasive morphological features as described by Cvetković et al. (2014). In summary, 35 mm Glass-bottom cell culture dishes (MatTek) were coated with 50% Matrigel (BD Bioscience) in serum-free medium. Once this layer solidified 2.5×10^4 cells seeded in 50% Matrigel in serum-free medium was placed above the initial layer, resulting in cells completely suspended in Matrigel. This 50% matrigel DMEM/F-12 serum-free medium was supplemented with DMSO (0.1%), U0126 (10 μM), or BB-94 (10 μM). Cell colony morphology was monitored for five days using bright-field microscopy (Leica DM16000 B microscope with Leica DFC425 camera) at 10X magnification, and representative 50 μm z-stack images (2 μm interval) taken at random locations across the matrix were captured using Leica MMAF software (Metamorph®). Fluorescent staining procedure was done as described in Cvetković et al. (2014) using Alexa Fluor 633 phalloidin (1:100) and DAPI (1 μg/mL) staining. Samples were imaged using a Nikon A1R+ confocal microscope and NIS Elements software (Nikon), capturing Z-stacks of approximately 100 μm. To analyze and score morphology of cell colonies, images representing a field of view at 20× magnification, were blindly analyzed using ImageJ software (NIH Bethesda). Protrusions were defined as thin extensions that emanated from a round cell colony. The number of protrusions on all cell colonies in an image was counted, with longer protrusions counted as multiples of the average protrusion length seen in that image to adjust for the heterogeneity in size observed. Disseminations were identified as small, round cells immediately adjacent to a larger colony. The score, representing the total number of protrusions or total number of disseminations for each treatment, was divided by the total number of colonies to arrive at the final measurement of protrusions or disseminations per colony.

Statistical analysis

Statistical analysis and graphing was performed using GraphPad Prism version 6.0. Data is presented as mean ± SEM, where all experiments were comprised of at least 3 biological replicates. One-way and Two-way ANOVA followed by Dunnett's post-hoc test were used and are indicated respectively in each figure legend. Different levels of statistical significance are denoted by a different number of asterisks and are as follows: ****, $p \leq 0.0001$, ***, $p \leq 0.001$, **, $p \leq 0.01$, *, $p \leq 0.05$, ns, $p < 0.05$.

Results

MT1-MMP expressing C2 and MDA-MB-231 cells facilitate a pERK mediated change in MMP-2 and MMP-9 levels.

To investigate the effect of MT1-MMP on ERK signalling and gelatinase levels, MCF-7 cells that stably express different levels of MT1-MMP were used. Parental MCF-7 cells, which are naturally MT1-MMP deficient (Kohrmann et al. 2009), and three stable clones that significantly differ in their stable expression of MT1-MMP transcript from high (C1, ~2500 fold compared to MCF-7 parental cells), medium (C2, ~1100 fold) to low (C3, ~11 fold) were used (Cepeda et al. 2016). As western blot analysis (Fig. 1a) demonstrated that cell line C2 had the highest level of pERK, most future work

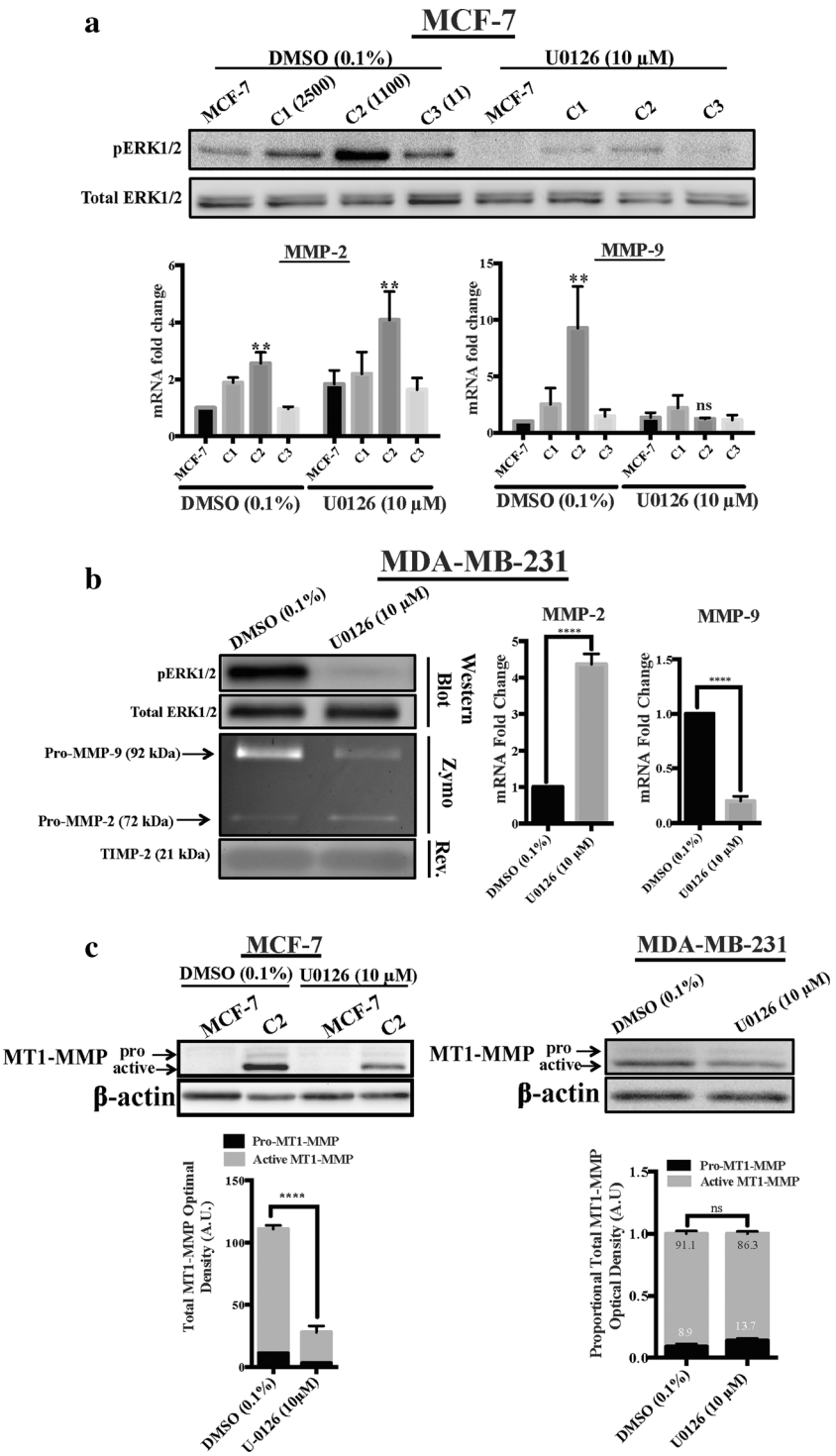

Fig. 1 MAPK signalling mediated an inverse relationship between MMP-2 and -9 expression in MT1-MMP positive breast cancer cells. **a)** Parental MCF-7 breast cancer cells, and MT1-MMP clonal cell lines (C1, C2, C3, see methods) were treated with the MAPK inhibitor U0126 (10 μM) and the levels of phospho-ERK were examined via immunoblot (top). The numbers in brackets indicate MT1-MMP mRNA fold change of clones relative to MCF-7 parental cells (=1). After U0126 treatment, the levels of MMP-2 and -9 mRNA were examined via qPCR and graphically displayed as mRNA fold change (bottom). **b)** MDA-MB 231 breast cancer cells were treated with U0126 (10 μM) and the protein levels of pERK, MMP-2, MMP-9, and TIMP-2 were analyzed via immunoblot, gelatin zymography, and reverse zymography, respectively (left). After U0126 treatment, the levels of MMP-2 and -9 mRNA were examined via qPCR and graphically displayed as mRNA fold change. **c)** MCF-7 together with MCF-7 C2 (left), and MDA-MB 231 (right) breast cancer cells were treated with U0126 (10 μM) and the levels of MT1-MMP protein were analyzed via immunoblot. Below the blots is the respective densitometry quantification of active and pro MT1-MMP protein normalized to β-actin levels. Means are presented ± SEM, and were compared using one-way ANOVA; ** $p < 0.01$; **** $p < 0.0001$

focused on this C2 line. C2 cells also had elevated MMP-2 and MMP-9 transcript levels compared to parental cells (Fig. 1a, left graph). The addition of the MEK inhibitor U0126 resulted in the decease of pERK in all cells, altered MMP-2 and -9 transcript levels (Fig. 1a), and also lowered MT1-MMP protein levels (Fig. 1c, left graph). This U0126 mediated decrease in MT1-MMP levels was mirrored by decreases in MMP-2 transcript levels, but opposite to an increase in MMP-9 transcript levels (Fig. 1a).

To corroborate the MCF-7 and C2 data, MDA-MB-231 cells were also used. Western blotting revealed that MDA-MB-231 contained pERK and active MT1-MMP protein, where pERK levels were reduced by U0126 (Fig. 1b). Zymography analysis of media removed from control MDA-MB-231 cells and those treated with U0126 demonstrated a decrease in proMMP-9 protein levels, but an increase in proMMP-2 (Fig. 1b). Reverse zymography showed that U0126 addition did not alter TIMP-2 protein levels from MDA-MB-231 cells (Fig. 1b). In agreement with the protein data, qPCR revealed a significant decrease in MMP-9 transcript levels, and an increase in MMP-2 transcripts (Fig. 1b). As with the C2 cells, and in agreement with the zymography data, MEK inhibition resulted in increased MMP-2, but decreased MMP-9 transcript levels in MDA-MB-231 cells (Fig. 1b right).

Western blot analysis and band intensity quantification also confirmed that while there is no active MT1-MMP in parental MCF-7 cells, the amount of active MT1-MMP protein in C2 cells was related to the levels of pERK (Fig. 1c). Treatment of C2 cells with U0126 significantly decreased the amount of active MT1-MMP protein in C2 cells, and while such U0126 treatment did decrease MT1-MMP levels in MDA-MB-231 cells, the decrease was not significant (Fig. 1c). Thus a pattern is seen with both C2 and MDA-MB-231 cells where MT1-MMP/pERK levels mirror MMP-2 levels, with MMP-9 always being opposite. Increasing active MT1-MMP level is mirrored by increased MMP-9 levels but accompanied by a decrease in MMP-2. Interestingly this inverse relationship is also seen in other cells in the context of MT1-MMP levels. Hs578T cells are MT1-MMP positive cells that endogenously produce low levels of pERK1/2, and as such display an inverse relationship regarding MMP-2 and -9 expression (data not shown) that relates to their low levels of pERK (Cepeda et al. 2016).

Inhibition of MMP activity, or interference of proMT1-MMP activation, in both C2 and MDA-MB-231 cells mediated an inverse relationship between MMP-2 and MMP-9 transcript levels.

Having seen a relationship between MT1-MMP, MMP-2 and MMP-9 levels we then sought to investigate the importance of the activity of MT1-MMP on the levels of MMP-2 and MMP-9. Parental MCF-7 cells, known to be MT1-MMP deficient, incubated with proMMP-2 containing media could not activate proMMP-2 protein (Fig. 2a). Conversely, C2 cells incubated with proMMP-2 containing media produced an active 63 kDa MMP-2 band, a band which was eliminated upon the addition of BB-94, demonstrating that this activation was dependent on MMP activity (Fig. 2a). Western blot analysis of MT1-MMP protein levels revealed that levels of active MT1-MMP present in C2 cells was increased significantly by BB-94 addition, but pERK levels were not (Fig. 2b and quantified below). qPCR showed significant increases in the levels of MT1-MMP and MMP-9 transcript levels in C2 cells treated with BB-94, but a significant decrease in MMP-2 (Fig. 2c). Western blot analysis of MDA-MB-231 cells treated with BB-94 MMP inhibitor displayed no change in pERK levels (as seen with C2 cells), and a non significant increase in the levels of active and inactive MT1-MMP protein (Fig. 2d and quantified to the right). In agreement with the trends seen with the protein data, qPCR revealed significant increases in MT1-MMP, and MMP-9 transcript levels, but a significant decrease in MMP-2 (Fig. 2e).

While the use of BB-94 allowed us to examine the necessity of MT1-MMP enzymatic activity, we next wanted to investigate the effect of altering the activation of proMT1-MMP using a furin inhibitor. As previously observed, Western bot analysis demonstrated no detectable levels of MT1-MMP in parental MCF-7 cells (Fig. 3a). However, while active MT1-MMP was present in C2 cells, the level was decreased in a dose-dependent manner by furin inhibitor – a pattern also seen for pERK levels in C2 cells (Fig. 3a). Quantification confirmed that furin significantly decreased both the level of active MT1-MMP protein and pERK levels (Fig. 3a graphs on right). In agreement with the observation that MMP-9 levels mirror that of active MT1-MMP, qPCR showed a significant decrease in MMP-9 transcript levels, but an increase in the levels of MMP-2 in C2 cells treated with furin inhibitor (Fig. 3b). Similarly, in MDA-MB-231 cells, the addition of furin inhibitor decreased, though not significantly, active MT1-MMP levels, and significantly decreased pERK levels (Fig. 3c and quantified to the right). qPCR analysis of these MDA-MB-231 cells revealed a significant decrease in MMP-9 transcript levels, but an increase in MMP-2 levels (Fig. 3d), again demonstrating the inverse relationship between MMP-2 and -9 mediated by MT1-MMP function.

MEK signalling inhibition decreased NF-κB transcription in C2 and MDA-MB-231 cells.

Towards investigating the inverse relationship between MMP-2 and MMP-9 transcript levels that are mediated by active MT1-MMP or pERK levels, a luciferase gene reporter assay was used to assess the transcriptional activity of AP-1 and NF-kB transcription factors. Treatment of parental MCF-7 cells with U0126 or BB94 did not alter AP-1 nor NF-kB transcription (Fig. 4a). Treatment of C2 cells with U0126 or BB94 did not alter transcription of AP-1, but the AP-1

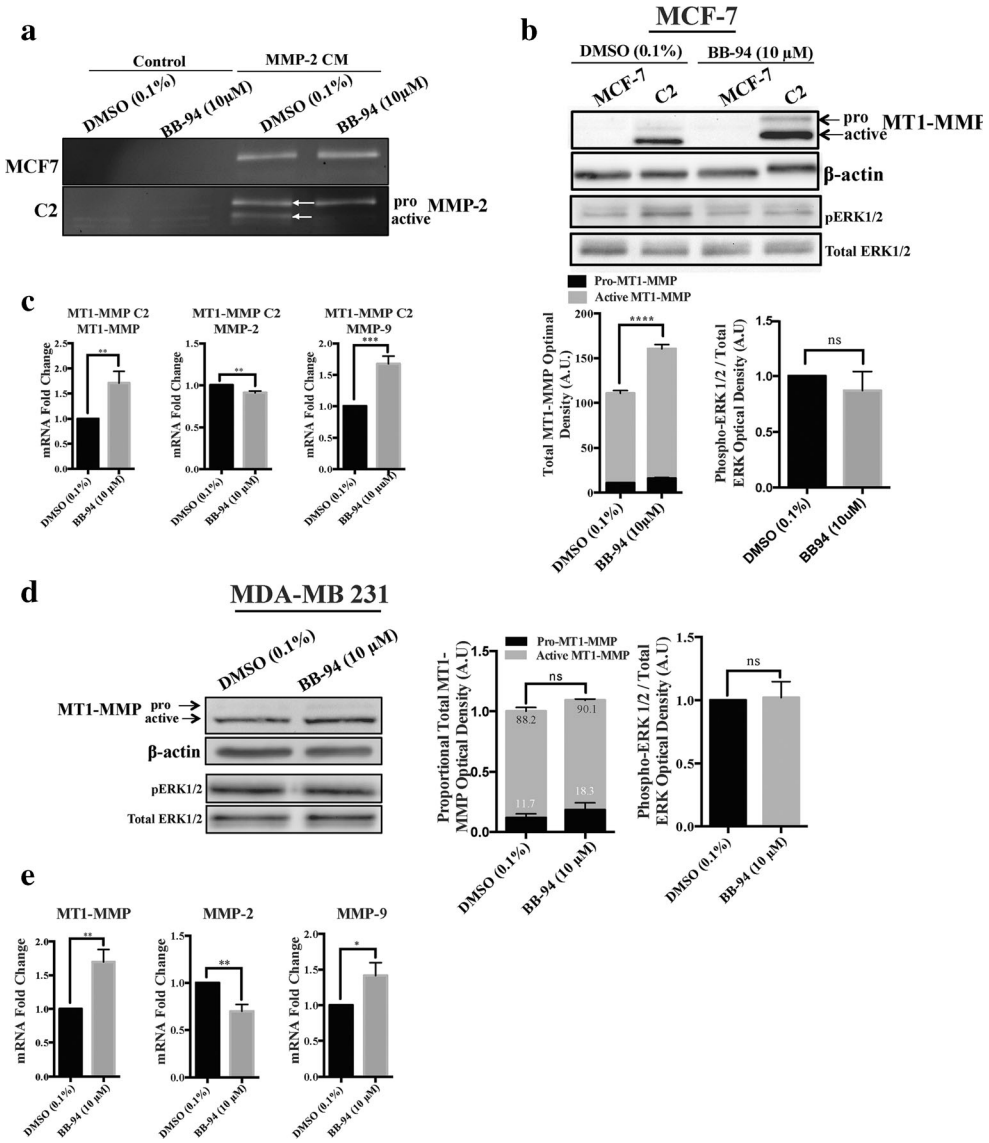

Fig. 2 BB-94 inhibition of MMP proteolytic activity caused a change in MMP-2/−9 and MT1-MMP transcript, but not pERK levels. **a)** MCF-7 and C2 cells were cultured in serum-free media (control) or with MMP-2 conditioned media (CM) and treated with DMSO (as a control) or BB-94 (10 μM) to analyze subsequent proMMP-2 activation via gelatin zymography. Only C2 cells were capable of proMMP-2 activation, as seen by presence of the active isoform of MMP-2, which was prevented with the incubation with BB-94. **b)** MCF-7 and C2 cells were treated with BB-94 (10 μM) and the levels of MT1-MMP and phospho-ERK protein were analyzed via immunoblot. Below the blots is the respective densitometry quantification of active and pro MT1-MMP, and phospho-ERK, normalized to β-actin and total ERK levels, respectively. **c)** MCF-7 and C2 cells were treated with BB-94 (10 μM) and the levels of MT1-MMP, MMP-2 and -9 mRNA were examined via qPCR and displayed as mRNA fold change. **d)** MDA-MB 231 cells were treated with BB-94 (10 μM) and the levels of MT1-MMP and phospho-ERK protein were analyzed via immunoblot. To the right of the blot are the respective densitometry quantification of active and pro MT1-MMP, and phospho-ERK, normalized to β-actin and total ERK levels, respectively. **e)** MDA-MB 231 cells were treated with BB-94 (10 μM) and the levels of MT1-MMP, MMP-2 and -9 mRNA were examined via qPCR and displayed as mRNA fold change. Means were presented ± SEM and analyzed via one-way ANOVA; * $p < 0.05$; ** $p < 0.01$; *** $p < 0.001$

transcription of C2 cells was significantly lower than the parental MCF-7 cells (Fig. 4a). Treatment of C2 cells with U0126 significantly decreased NF-kB transcription (Fig. 4a). MDA-MB-231 cells treated with U0126 or BB94 did not alter AP-1 transcription (Fig. 4b), however, treatment with U0126 (but not BB94) significantly decreased NF-kB transcription in MDA-MB-231 cells (Fig. 4b bottom).

Inhibition of MAPK signalling activity inhibited both the migration and invasion of MDA-MB-231 cells, while BB-94 inhibition of MMP activity only inhibited invasion.

Having demonstrated that both C2 and MDA-MB-231 cells alter MT1-MMP and MMP-9 levels in a similar pattern, always being opposite than that of MMP-2, we then wanted to investigate how such MMP differences would manifest themselves

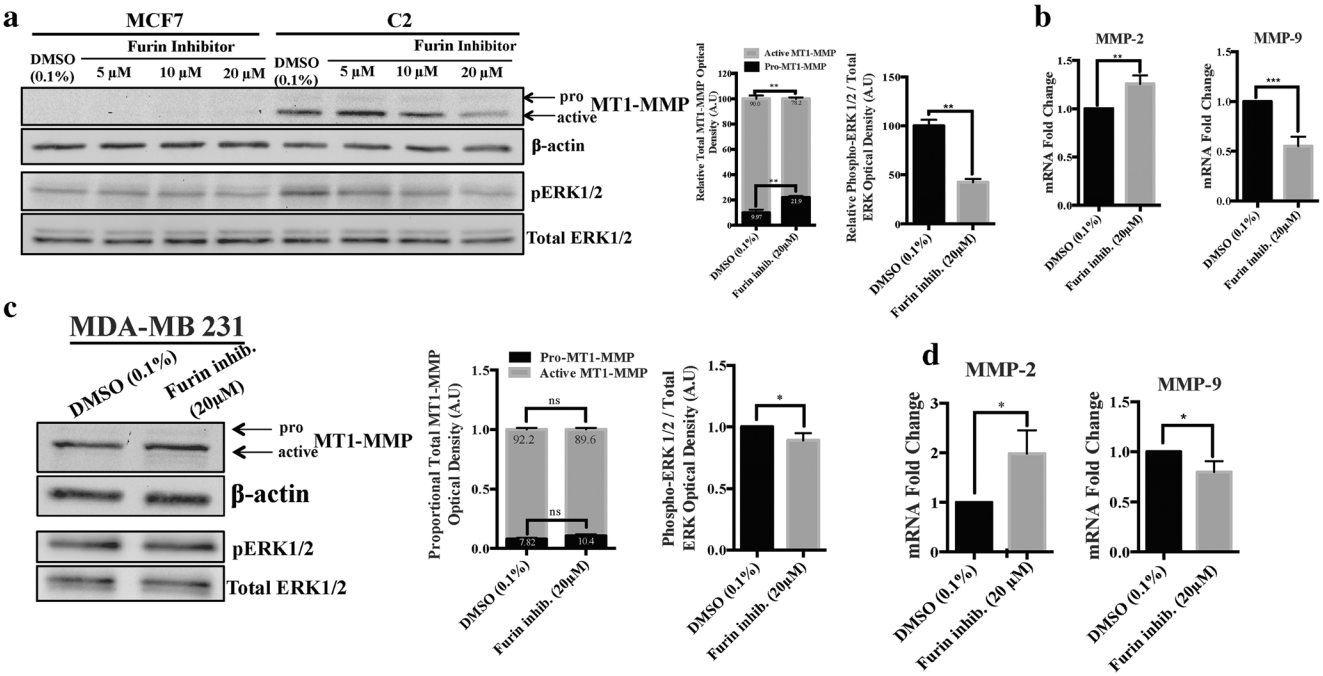

Fig. 3 Interference of MT1-MMP activation caused a change in MMP-2/−9 expression. **a)** MCF-7 and C2 cells were treated with a furin inhibitor (5,10, and 20 μM) and the levels of MT1-MMP and phospho-ERK protein were analyzed via immunoblot. To the right is the respective densitometry quantification of active and pro MT1-MMP, and phospho-ERK, normalized to β-actin and total ERK levels, respectively. **b)** MCF-7 and C2 cells were treated with a furin inhibitor (20 μM) and the levels of MMP-2 and -9 mRNA were examined via qPCR and displayed as mRNA fold change. Means were presented ± SEM and analyzed via one-way ANOVA. **c)** MDA-MB 231 cells were treated a furin inhibitor (20 μM) and the levels of MT1-MMP and phospho-ERK protein were analyzed via immunoblot. To the right is the respective densitometry quantification of active and pro MT1-MMP, and phospho-ERK, normalized to β-actin and total ERK levels, respectively. **d)** MDA-MB 231 cells were treated with a furin inhibitor (20 μM) and the levels of MMP-2 and -9 mRNA were examined via qPCR and displayed as mRNA fold change. Means were presented ± SEM and analyzed via one-way ANOVA; * $p < 0.05$; ** $p < 0.01$; *** $p < 0.001$

in modulating cell movement. MDA-MB-231 cells were used as this cell line's invasive properties have been well characterized. Confluent MDA-MB-231 cells were subject to a scratch-wound-closure assay. Following the initial "wound", DMSO, U0126, and BB94 treated cells all migrated to close the wound to a similar state at 24 h; however, at the 12-h time point, U0126 treated cells showed a significant delay in migration and wound closure (Fig. 5a). Cell migration was also measured via movement of cells through an 8 μm transwell pore. The addition of U0126, but not BB-94, reduced the number of MDA-MB-231 cells that migrated through the transwell (Fig. 5b). A similar assay was used where Matrigel was used to coat the transwell pores, thus cell invasion was dependent on degradation of the ECM. Both addition of U0126 and BB-94 reduced the number of MDA-MB-231 cells that invaded through the pore, though the addition of U0126 had a greater affect (Fig. 5c).

Inhibition of MAPK signalling and MMP activity both decreased the number of cell protrusions, and both increased the number of cellular blebs of MDA-MB-231 cells in 3D Matrigel culture.

We wanted to account for any unintended cell structural changes that may have occurred due to altered ERK signalling or MMP enzymatic activity after addition of the MEK inhibitor U0126 and the MMP inhibitor BB-94. To examine changes in cell morphology that are relevant to cell movement, MDA-MB-231 cells were embedded in Matrigel and treated with U0126 or BB-94. By Day 5, morphological differences were apparent (Fig. 6a). MDA-MB-231 cells treated with U0126 or BB-94 were significantly less protrusive (~ 2–3 protrusions per colony) than vehicle treated MDA-MB-231 cells (~9 per colony) (Fig. 6a, and quantified in b). Alternatively, MDA-MB-231 cells treated with U0126 or BB94 all had significantly more disseminations (Fig. 6a, and quantified in b). Immunofluorescence analysis examining nuclear and actin stains in these cells revealed that control MDA-MB-231 cells were a network of elongated cells. Inhibition by U0126 abolished the ability to form elongated processes, resulting in small round single cells with very concentrated F-actin. Inhibition of MMP catalytic activity with BB-94 resulted in distinctly large aggregations of round cells, though some BB-94 treated MDA-MB-231 cells were still able to elongate (Fig. 6c).

Discussion

This study aimed to characterize the functional consequences of an observed inverse relationship between MMP-2 and -9 transcript levels as they related to MT1-MMP function. We examined the effects of MT1-MMP proteolytic and non-

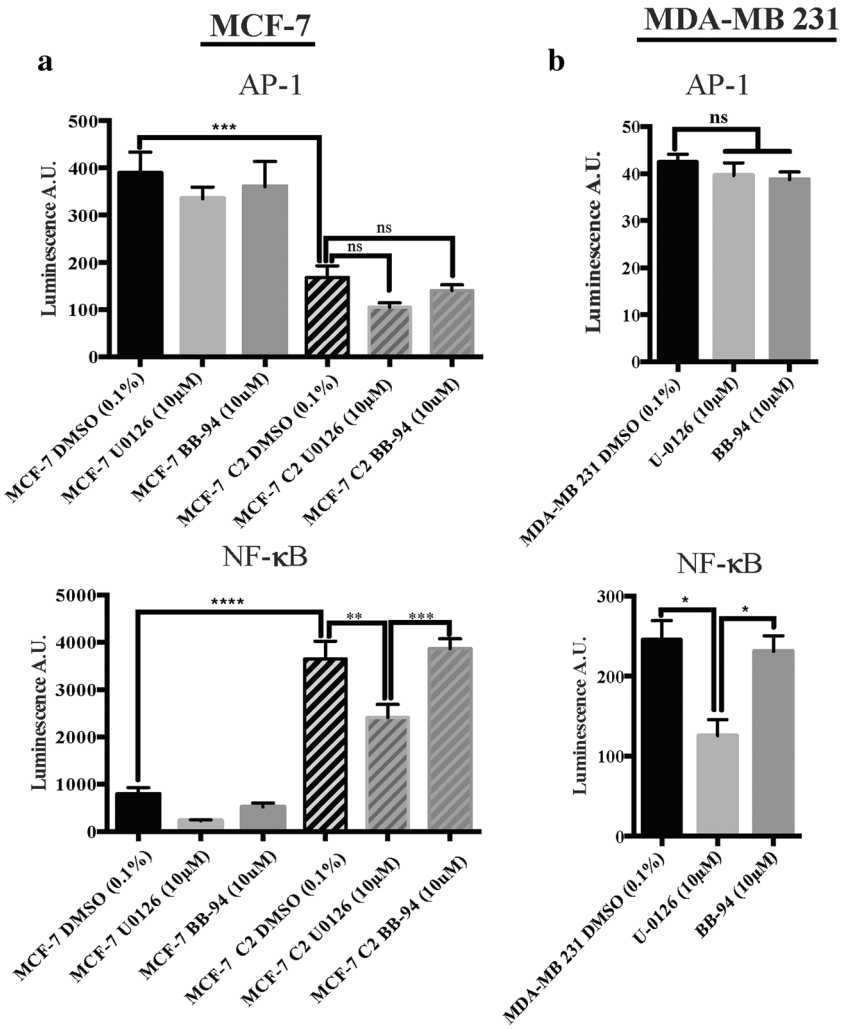

Fig. 4 MT1-MMP expressing breast cancer cells demonstrated differential activity of AP-1 and NF-κB transcription factors. MCF-7 and C2 cells **(a)** or MDA-MB 231 cells (**b**) were transfected with luciferase constructs controlled by either the AP-1 (left) or NF-κB (right) promoter and treated with DMSO (as a control), U0126, or BB-94 (10 μM). Following treatment, cells were lysed and the levels of luciferin produced was quantified using a luminometer. Data is displayed as mean luminescence (a.u.) ± SEM and analyzed via one-way ANOVA; * $p < 0.05$; ** $p < 0.01$; *** $p < 0.001$; **** $p < 0.0001$. Note how U0126 treatment only affects NF-κB activity in MT1-MMP positive breast cancer cells

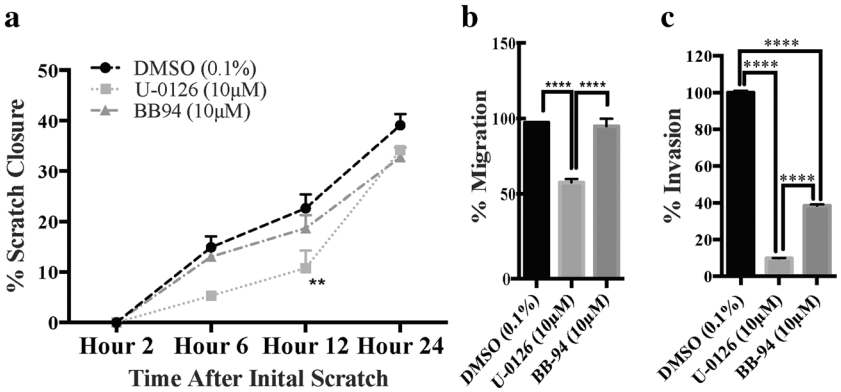

Fig. 5 Inhibition of MAPK signalling and MMP activity decreased the migratory ability of MDA-MB 231 cells**. a)** MDA-MB 231 cells were seeded on a culture dish and allowed to reach confluency. Afterwards a scratch was created in the middle of the monolayer, cell debris was washed, and cells were incubated in media containing DMSO (as a control), U0126 or BB-94 (10 μM) for 24 h. During this incubation period, the closure of the scratch was monitored using brightfield microscopy. Scratch closure was quantified every day by measuring the distance of migration using ImageJ and normalizing it to the initial scratch size. **b,c)** MDA-MB 231 cells were treated with DMSO (as a control), U0126 or BB-94 (10 μM) and plated on the upper surface of an uncoated transwell insert (**b**, migration) or an insert coated with 20% matrigel (**c**, invasion) in media without serum and allowed to migrate for 12 h to the bottom compartment that contains media with 10% FBS. Cells that migrated to the bottom compartment were quantified and displayed as relative migration to MDA-MB 231 cells incubated with 0.1% DMSO. Means are presented ± SEM, and were compared using one-way ANOVA; ** $p \leq 0.01$; **** $p < 0.0001$

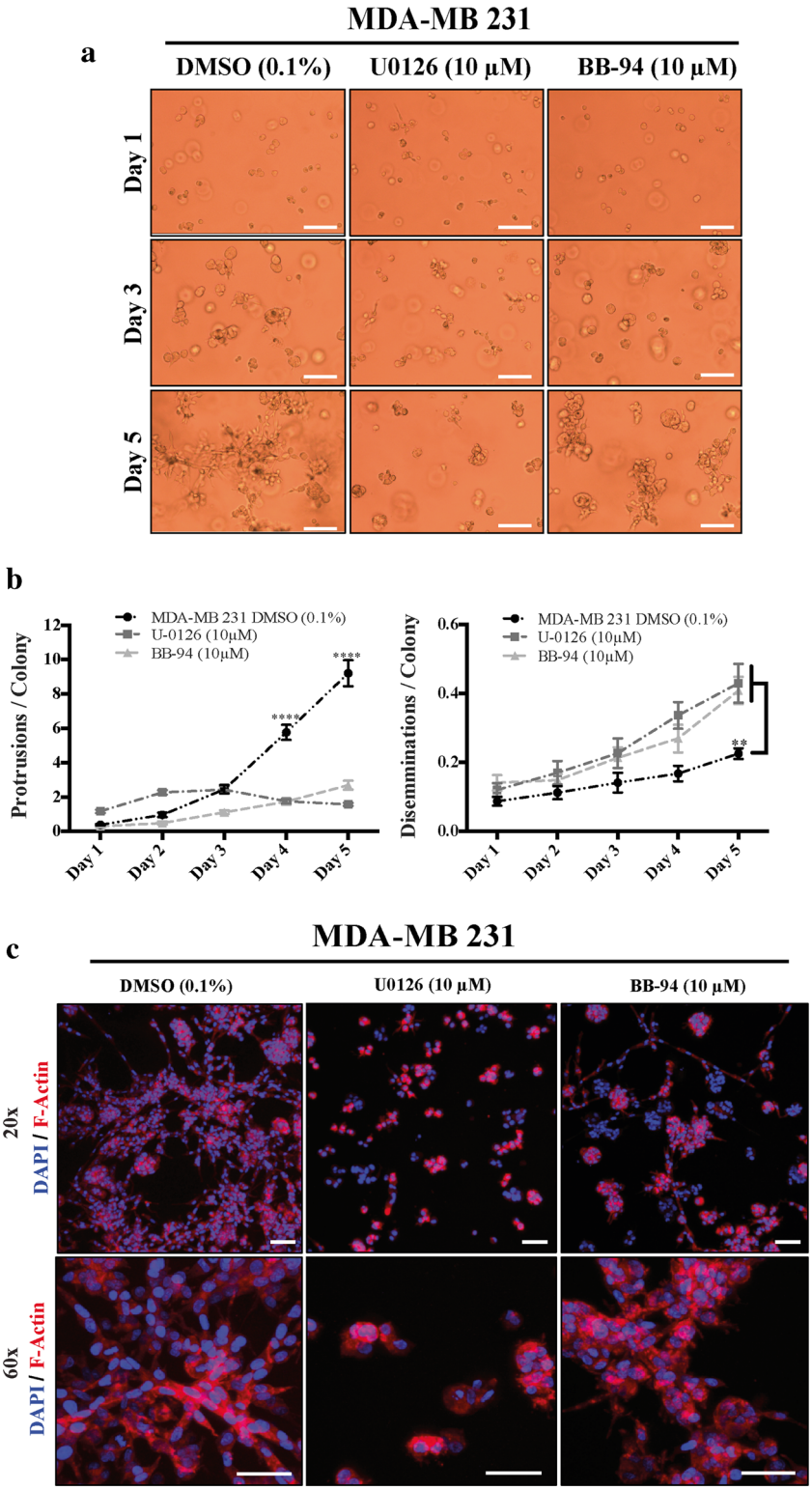

Fig. 6 Inhibition of MAPK signalling and MMP activity inhibited a protrusive phenotype in Matrigel 3D culture. **a)** Brightfield images of MDA-MB 231 cells 1, 3, and 5 days after being embedded in Matrigel and incubated in media containing 10% FBS supplemented with DMSO (as a control), U0126 or BB-94 (10 µM). *Scale bars* = 100 µm. **b)** The number of protrusions (*left*) or disseminations (*right*) per colony for each treatment was blindly quantified every day for 5 days during 3D culture. Means are presented ± SEM, and were compared using one-way ANOVA; **, $p \leq 0.01$; ****, $p \leq 0.0001$. **c)** Immunofluorescence analysis of MDA-MB 231 cells 5 days after being embedded in Matrigel and incubated with DMSO (as a control), U0126 or BB-94 (10 µM). Shown is a 3D volume view merge at 20X (*top*) and 60× (*bottom*) of DAPI (*blue*) and F-actin channels (*red*). Scale bars = 100 µm

proteolytic functions on orchestrating the movement of cells by manipulating MT1-MMP activation (furin inhibitor), MMP catalytic activity (BB-94), and ERK phosphorylation (U0126). We used MCF-7 cells, which have low levels of MT1-MMP and pERK (Kohrmann et al. 2009) as well as a manipulated cell line (C2) and MDA-MB-231 cells, both of which have relatively high levels of active MT1-MMP and pERK (Cepeda et al. 2016; Kohrmann et al. 2009). Increased active MT1-MMP proteins levels were always associated with increased pERK levels and increased MMP-9

transcript levels, but with reduced MMP-2 transcript levels. Moreover, cells with active MT1-MMP facilitated ERK phosphorylation and subsequent transcriptional activity of NF-κB. Our results describe that inhibiting proMT1-MMP activation, MMP activity, and/or ERK1/2 phosphorylation always resulted in an inverse change between MMP-2 and MMP-9 transcript levels. BB-94 treatment to inhibit MMP activity did not significantly alter cell migration, though inhibition of ERK1/2 phosphorylation did. Conversely, both inhibition of ERK1/2 phosphorylation and MMP activity did inhibit cell invasion.

Proper ERK1/2 signalling is essential in many cellular processes including migration, proliferation, and apoptosis (Fujioka et al. 2006). Subsequently, pERK can influence transcription factors, known to regulate the transcription of a broad number of MMPs, with NF-κB, shown to specifically regulate MT1-MMP and MMP-9, but not MMP-2 (Overall and Lopez-Otin 2002). In this study, inhibiting ERK1/2 phosphorylation in both C2 and MDA-MB-231 cells resulted in increased MMP-2, but decreased MMP-9 mRNA levels (Fig. 1 and data not shown), indicating that the relationship is conserved, at least between C2 and MDA-MB-231 cells. Inhibition of ERK1/2 phosphorylation in C2 and MDA-MB-231 cells also resulted in decreased NF-κB transcriptional activity (Fig. 4), providing support for a role in pERK regulation of MMP-9 expression. A similar study performed by Lee et al. (2013) in bladder cancer cells demonstrated that with inhibition of ERK1/2 phosphorylation, both NF-κB transcriptional activity and MMP-9 expression decreased. Tandem decreases in MMP-9 and MT1-MMP mRNA levels following inhibition of ERK1/2 phosphorylation have also been previously observed in rhabdomyosarcoma, fibrosarcoma, bladder, colon, and prostate carcinoma cells (Tanimura et al. 2003).

In addition to being capable of regulating MMP transcript levels, pERK influences a multitude of genes whose products control the cytoskeleton, receptors, cytokines and growth factors. Inhibition of ERK1/2 phosphorylation in MDA-MB-231 cells resulted in decreased cell migration as measured by scratch closure and transwell migration assays as well as decreased invasion through a Matrigel coated transwell (Fig. 5). This alone does not directly support a role for MT1-MMP in cell movement, but does support previous work reporting the necessity of proper pERK signalling in order to achieve cell migration and invasion (Meloche and Pouysségur 2007). Towards better understanding the role pERK levels may play in cell movement in an MT1-MMP-dependent context, cell morphology was also examined. Acquisition of an invasive phenotype requires modulation of cell-ECM interactions through cytoskeletal organization, proteolysis of the extracellular matrix, and migration (Friedl and Wolf 2003). Upon inhibition of ERK1/2 phosphorylation in 3D cell culture, the morphology of MDA-MB-231 breast cancer cells changed to become round with a minimally protrusive phenotype. Fluorescence microscopy revealed a condensed and aggregated F-actin cytoskeletal network, contrasting that which forms in untreated cells (Fig. 6). The reduction of protrusions following treatment with U0126 could be attributed to deficiency in cytoskeletal organization as the formation of invadopodia requires actin polymerization to form a membrane protrusion that contains MT1-MMP at the distal end (Artym 2006). Here, cells with decreased pERK levels trend towards decreased active MT1-MMP and proMMP-9 protein levels. With a reduction of MT1-MMP protein there is less ability to form functional invadopodia. Further, MT1-MMP-mediated proMMP-2 activation would also be reduced, consequently reducing the activation of proMMP-9. Therefore, cells with decreased pERK may have a lowered ability to form invadopodia and lowered ability to degrade ECM constituents as evidenced by reduced invasion through Matrigel coated transwells.

Inhibition of MMP catalytic activity by BB94 in both C2 and MDA-MB-231 cells resulted in an increase in MT1-MMP and MMP-9 transcript levels (Fig. 2), but decreased MMP-2 mRNA. In agreement with increased transcript levels, BB-94 inhibition also increased the level of active MT1-MMP protein, though this increase was not significant. While addition of BB-94 would result in inhibition of MMP catalytic activity, this inhibition of the catalytic domain of MT1-MMP does not prevent signal transduction (D'Alessio et al. 2008; Sounni et al. 2010). Thus, despite MMP catalytic inhibition, MAPK activation can still occur, whereby subsequent activity of pERK could be increasing the expression of MT1-MMP in both C2 and MDA-MB-231 cells. This increase in MT1-MMP transcript is not a result of transcriptional activity of transcription factors AP-1 or NF-κB (Fig. 4), as their activity was not altered in the presence of BB-94. MT1-MMP transcriptional control is unique amongst MMP family members due to differences in its promoter sequence, though pERK mediated activation is often involved (Lohi et al. 2000; Sroka et al. 2007). MDA-MB-231 cells are invasive cells that upon treatment with MMP inhibitor BB-94, they drastically decreased their invasion through a Matrigel coated transwell barrier (Fig. 5) and displayed a less protrusive phenotype in 3D cell culture (Fig. 6). Intriguingly, unlike treatment with U0126, the migratory ability of these cells is not impaired by BB94. This maintenance of pERK levels could preserve cell migratory machinery, but as migration alone does not require degradation of ECM constituents, the changes observed in MMP-2 and MMP-9 transcript levels are assumed to not impact this cell motility event. Invasion on the other hand, was considerably impacted by inhibition of all MMP catalytic activity. This is evident based on decreased transwell invasion (Fig. 5) and a noticeably less protrusive phenotype in 3D culture (Fig. 6).

Active MT1-MMP present on the cell surface is in part dependent on intracellular activation of proMT1-MMP within the Golgi and trans-Golgi network through a protein convertase called furin (Seidah et al. 2008). Following treatment with Furin Inhibitor I, C2 cells exhibited an increase in

proMT1-MMP levels, and an associated decrease in active MT1-MMP levels, as well as decreased pERK protein levels (Fig. 3). Furin inhibition in MDA-MB-21 cells, did not significantly alter MT1-MMP protein levels, but the trend was an increase in proMT1-MMP levels, and an associated decrease in active MT1-MMP as expected with inhibition of activation of the pro-form. As with the C2 cells, furin inhibition did result in decreased pERK levels. In addition to the decrease in pERK levels seen after inhibition of furin in both C2 and MDA-MB-231, this inhibition resulted in a decrease in MMP-9 transcript levels, but increased MMP-2 transcript levels. The consistency between the two cell lines regarding decreased pERK signalling and associated decreases in MMP-9 transcript levels, but increases in MMP-2 levels, demonstrates a conserved mechanism for influencing MMP-2/−9 expression.

In this study, furin inhibition linked proMT1-MMP activation to an inverse expression of the gelatinase genes. Similarly, BB94 inhibition of MMP activity and U0126 inhibition of ERK phosphorylation resulted in an inverse expression of the gelatinase genes. As the levels of active MT1-MMP have an affect on the enzymatic activity of other MMPs and ERK phosphorylation, MT1-MMP is positioned as an important player in coordinating both enzymatic events, cell signalling cascades, and a functional transcriptional network with MMP-2 and -9 that may be required for cell migration and invasion.

References

Artym VV (2006) Dynamic interactions of cortactin and membrane type 1 matrix metalloproteinase at invadopodia: defining the stages of invadopodia formation and function. Cancer Res 66(6):3034–3043

Assent D, Bourgot I, Hennuy B, Geurts P, Noel A, Foidart JM, Maquoi E (2015) A membrane-type-1 matrix metalloproteinase (MT1-MMP)-discoidin domain receptor 1 axis regulates collagen-induced apoptosis in breast cancer cells. PLoS One 10(3):e0116006

Bateman JF, Boot-Handform RP, Lamandé SR (2009) Genetic diseases of connective tissues: cellular and extracellular effects of ECM mutations. *Nature Reviews*. Genetics 10(3):173–183

Bourboulia D, Stetler-Stevenson WG (2010) Matrix metalloproteinases (MMPs) and tissue inhibitors of metalloproteinases (TIMPs): positive and negative regulators in tumour cell adhesion. Semin Cancer Biol 20(3):161–168

Cepeda M, Pelling J, Evered C, Williams K, Freedman Z, Stan I, Willson J, Leong H, Damjanovski S (2016) Low expression of MT1-MMP is optimal to promote tumourigenesis of breast cancer cells and is not associated with widespread ECM degradation. BMC Molecular Cancer 15:65

Coppola JM, Bhojani MS, Ross BD, Rehemtulla A (2008) A small-molecule furin inhibitor inhibits cancer cell motility. Neoplasia 10(4):363–370

Cvetković D, Goertzen CG-F, Bhattacharya M (2014) Quantification of breast cancer cell invasiveness using a three-dimensional (3D) model. J Vis Exp: JoVE (88). https://www.jove.com/video/51341/quantification-breast-cancer-cell-invasiveness-using-three

D'Alessio S, Ferrari G, Cinnante K, Scheerer W, Galloway AC, Roses DF, Rozanov DV, Remacle AG, Oh ES, Shiryaev SA, Strongin AY, Pintucci G, Mignatti P (2008) Tissue inhibitor of metalloproteinases-2 binding to membrane- type 1 matrix metalloproteinase induces MAPK activation and cell growth by a non-proteolytic mechanism. J Biol Chem 283(1):87–99

DeSilva DR, Jones EA, Favata MF, Jaffee BD, Magolda RL, Trzaskos JM, Scherle PA (1998) Inhibition of mitogen-activated protein kinase kinase blocks T cell proliferation but does not induce or prevent Anergy. J Immunol 160(9):4175–4181

Frantz C, Stewart KM, Weaver VM (2010) The extracellular matrix at a glance. J Cell Sci 123:4195–4200

Friedl P, Wolf K (2003) Tumour-cell invasion and migration: diversity and escape mechanisms. *Nature Reviews*. Cancer 3(5):362–374

Fujioka A, Terai K, Itoh RE, Aoki K, Nakamura T, Kuroda S, Nishida E, Matsuda M (2006) Dynamics of the Ras/ERK MAPK Cascade as monitored by fluorescent probes. J Biol Chem 281(13):8917–8926

Hotary K, Li XY, Allen E, Stevens SL, Weiss SJ (2006) A cancer cell Metalloprotease triad regulates the basement membrane transmigration program. Genes Dev 20(19):2673–2686

Hynes RO, Naba A (2012) Overview of the Matrisome-an inventory of extracellular matrix constituents and functions. Cold Spring Harb Perspect Biol 4(1):1–16

Itoh Y, Takamura A, Ito N, Maru Y, Sato H, Suenaga N, Aoki T, Seiki M (2001) Homophilic complex formation of MT1-MMP facilitates proMMP-2 activation on the cell surface and promotes tumour cell invasion. EMBO J 20(17):4782–4793

Järveläinen H (2009) Extracellular matrix molecules: potential targets in pharmacotherapy. Pharmacology Reviews 61(2):198–223

Klein T, Bischoff R (2011) Physiology and pathophysiology of matrix Metalloproteases. Amino Acids 41(2):271–290

Kohrmann A et al (2009) Expression of matrix metalloproteinases (MMPs) in primary human breast cancer and breast cancer cell lines: new findings and review of the literature. BMC Cancer 9:188

Lambert E, Bernard Haye D, Petitfrère E (2004) TIMPs as Multifacial proteins. Crit Rev Oncol Hematol 49(3):187–198

Lee SJ, Cho SC, Lee EJ, Kim S, Lee SB, Lim JH, Choi YH, Kim WJ, Moon SK (2013) Interleukin-20 promotes migration of bladder cancer cells through extracellular signal-regulated kinase (Erk)-mediated Mmp-9 protein expression leading to nuclear factor (Nf-kb) activation by inducing the up-regulation of p21waf1 protein expression. J Biol Chem 288(8):5539–5552

Lehti K, Valtanen H, Wickström S, Lohi J, Keski-Oja J (2000) Regulation of membrane-type-1 matrix metalloproteinase activity by its cytoplasmic domain. J Biol Chem 275(20):1506–1513

Lohi J, Lehti K, Valtanen H, Parks WC, Keski-Oja J (2000) Strutural analysis and promoter characterization of the human membrane- type matrix metalloproteinase-1 (MT1-MMP) gene. Gene 242(1):75–86

Low A, Bone A, Johnson D, Dickson B (1996) The matrix metalloproteinase inhibitor Batimastat (BB-94) retards human breast cancer solid tumour growth but not ascites formation in nude mice. Clin Cancer Res 2(1):1207–1215

Marshall J (2011) Transwell (®) invasion assays. Methods in molecular biology 769:97–110. doi:10.1007/978-1-61779-207-6_8

Meloche S, Pouysségur J (2007) The ERK1/2 mitogen-activated protein kinase pathway as a master regulator of the G1- to S-phase transition. Oncogene 26(22):3227–3239

Mori H, Tomari T, Koshikawa N, Kajita M, Itoh Y, Sato H, Tojo H, Yana I, Seiki M (2002) CD44 directs membrane-type 1 matrix metalloproteinase to lamellipodia by associating with its hemopexin-like domain. EMBO J 21(15):3949–3959

Overall CM, Lopez-Otin C (2002) Strategies for MMP inhibition in cancer: innovations for the post-trial era. Nature Reviews 2(1):657–672

Pahwa S, Stawikowski MJ, Fields GB (2014) Monitoring and inhibiting MT1-MMP during cancer initiation and progression. Cancers 6(1):416–435

Poincloux R, Lizárraga F, Chavrier P (2009) Matrix invasion by tumour cells: a focus on MT1-MMP TRAFficking to invadopodia. J Cell Sci 122(17):3015–3024

Sabeh F, Li XY, Saunders TL, Rowe RG, Weiss SJ (2009) Secreted versus membrane-anchored collagenases: relative roles in fibroblast-dependent Collagenolysis and invasion. J Biol Chem 284(34):23001–23011

Seidah NG, Mayer G, Zaid A, Rousselet E, Nassoury N, Poirier S, Essalmani R, Prat A (2008) The activation and physiological functions of the Proprotein Convertases. Int J Biochem Cell Biol 40(6–7):1111–1125

Sounni NE, Rozanov DV, Remacle AG, Golubkov VS, Noel A, Strongin AY (2010) Timp-2 binding with cellular MT1-MMP stimulates invasion-promoting MEK/ERK signalling in cancer cells. Int J Cancer 126(5):1067–1078

Sroka IC, Nagle RB, Bowden GT (2007) Membrane-type 1 matrix metalloproteinase is regulated by Sp1 through the differential activation of AKT, JNK, and ERK pathways in human prostate tumor cells. Neoplasia 9(5):406–417

Sternlicht MD, Werb Z (2001) How matrix metalloproteinases regulate cell behavior. Annu Rev Cell Dev Biol 17(1):463–516

Tanimura S, Asato K, Fujishiro S, Kohno M (2003) Specific blockade of the ERK pathway inhibits the invasiveness of tumor cells: down-regulation of matrix metalloproteinase-3/−9/−14 and CD44. Biochem Biophys Res Commun 304(1):801–807

Toth M, Sohail A, Fridman R (2001) Assessment of gelatinases (MMP-2 and MMP-9) by gelatin zymography. Methods in Molecular Medicine 878(1):121–135

Toth M, Chvyrkova I, Bernardo MM, Hernandez-Barrantes S, Fridman R (2003) Pro-MMP-9 activation by the MT1-MMP/MMP-2 axis and MMP-3: role of TIMP-2 and plasma membranes. Biochem Biophys Res Commun 308(1): 386–395